

DEVELOPMENT OF A FIBER-OPTIC BEAM LOSS POSITION MONITOR FOR THE ADVANCED PHOTON SOURCE STORAGE RING*

J. C. Dooling[†], W. Berg, L. Emery, and B.-X. Yang, ANL, Argonne, IL 60439, USA

Abstract

An array of fused-silica, fiber optic bundles has been built to spatially monitor e-beam loss in the APS storage ring (SR). A prototype beam loss position monitor (BLPM) has been installed on unoccupied undulator straight sections. The BLPM allows for 6 fiber bundles, 3 above and 3 below the beam. The center bundles are aligned with the beam axis. Presently, 4 bundles are used, 3 above and one in the center position below the beam. Each bundle is 3 m in length and composed of 61 220- μm -diameter fibers for a total aperture of 2 mm. The first 30 cm of each bundle are aligned parallel to the beam in contact with the vacuum chamber. The rest of the fiber acts as a light pipe to transmit photons to shielded PMTs. Tests show good signal strength during stored-beam mode from Touschek scattering and deterministic losses that occur during top-up injection and beam dumps. Light generated by fast electrons within the fibers is thought to come primarily from Cherenkov radiation. Post-injection loss signals show spatial and temporal dynamics. Simulation work is expected to provide calibration for integrated losses that can be compared with progressive undulator demagnetization.

INTRODUCTION

Beam losses from electron machines such as the Advanced Photon Source (APS) storage ring (SR) can result in damage to the permanent magnets used to generate x-ray photons. Regardless of the cause of damage, all the energy that can potentially affect the magnets is initially carried by fast electrons, therefore monitoring their loss, in close proximity to the undulators is necessary.

Detection of electrons can be accomplished through several mechanisms including Cherenkov radiation (CR) and optical transition radiation (OTR). The reduction in transmission of glass or plastic fiber optic (FO) cable is itself used as a form of radiation detection in some applications [1]. On the other hand, fused silica (SiO_2) is radiation resistant to very high dose levels. Cylindrical volumes of fused silica are presently employed in the APS Cherenkov detectors (CDs) located in most undulator straight sections of the SR [2]. In addition, fused-silica optical fibers have been suggested for use in detecting beam losses from high-energy electron [3] and proton [4] machines.

High-energy electrons lost from the beam continue to travel mainly in the direction of the beam. Optical fiber is positioned with the axis parallel to the beam on the surface

of the beam vacuum chamber. The angular extent of the OTR light cone for high-gamma electrons is small and is totally internally reflected within the fiber. Using the same physical model, where lost electrons are again traveling approximately parallel to the beam, the light generated from Cherenkov radiation will have a much larger light cone angle, and total internal reflection would not occur within the fiber. OTR lobes occur on both sides of the index transition, so a reflector can be used at the upstream end of the fiber to increase intensity [5]. In addition, the reflector creates its own OTR radiation with the passage of an electron. A comparison of OTR and Cherenkov radiation is shown in Figures 1 and 2. Cherenkov radiation is a volume process, whereas OTR occurs at a surface between regions of different refractive indices. Because it is a surface process, OTR also occurs along the barrel of the fiber bundle as illustrated in Figure 3.

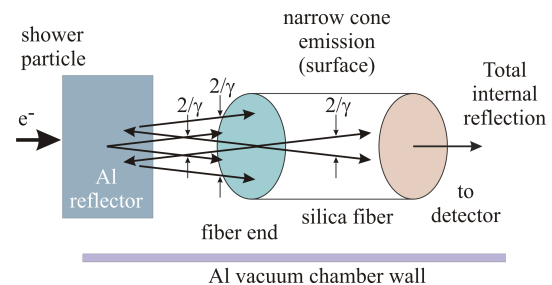


Figure 1: Fiber OTR with upstream end reflector.

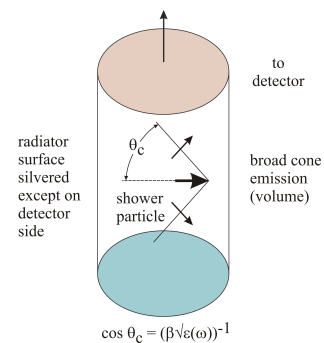


Figure 2: APS Cherenkov radiation detector.

ANALYSIS

We compare directly the signals from Cherenkov and OTR processes for a given flux of lost electrons Γ_e . Based on the complex geometries involved, the following calculations can only be approximations. A more accurate estimate of signal strength and dose requires simulation. This work is on going.

* Work supported by the U.S. D.O.E., Office of Science, Office of Basic Energy Sciences, under contract number DE-AC02-06CH11357.

[†] dooling@aps.anl.gov

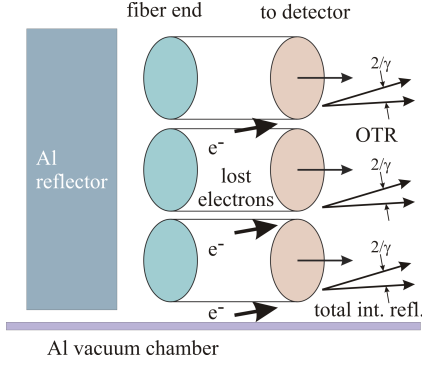


Figure 3: FO bundle OTR with side penetration.

Cherenkov

Cherenkov radiation occurs when an electron travels through a medium at a speed in excess of the speed of light in that medium, $v = \beta/n(\omega)$, where $n(\omega)$ is the frequency-dependent index of refraction. In fused silica, the index varies slightly with photon wavelength λ ; for $\lambda=500$ nm, $n=1.46$. CR will then occur when the normalized electron velocity $\beta > n(\omega)^{-1}=0.685$, corresponding to a kinetic energy of 0.19 MeV ($\gamma=1.37$). However, to fully penetrate the radiator medium, electron energies should be in excess of approximately 4 MeV. At 4 MeV $\beta=0.994$, and the angle of photon emission or light cone angle [6] $\theta_c = \cos^{-1}(1/(\beta n(\omega))) = 46.4^\circ$. The light cone angle varies only slightly up to the maximum energy of the electron (7 GeV in the APS, $\theta_c = 46.8^\circ$). CR intensity from a single electron per differential path length and frequency can be determined using the Frank-Tamm expression [7]:

$$\frac{d^2 E_{CR}}{dx d\omega} = \frac{e^2 \mu(\omega)}{4\pi} \omega \left[1 - \frac{1}{\beta^2 n^2(\omega)} \right] \quad (1)$$

where e is the electron charge, and $\mu(\omega)$ is the frequency-dependent permeability of the medium. Ignoring the energy dependence which is weak above 2 MeV, the total number of CR photons is obtained as follows,

$$d^2 N_{CR} = \frac{d^2 E_{CR}}{\hbar\omega} = \frac{\mu(\omega)e^2}{4\pi\hbar} \left(1 - \frac{1}{\beta^2 n^2} \right) d\omega dx. \quad (2)$$

Over the frequency range of interest (wavelength range from 320 nm to 650 nm), the refractive index varies from 1.483 to 1.457, so a constant value of 1.47 is chosen. In addition, no magnetic materials are used; therefore $\mu(\omega) = \mu_r(\omega)\mu_o = \mu_o$. The frequency range is determined by the response of the photomultiplier tubes (PMTs) discussed below. Integrating over the frequency, converting to wavelength $\lambda = 2\pi c/\omega$, and introducing the fine structure constant $\alpha = e^2/4\pi\epsilon_o\hbar c$, we obtain

$$\begin{aligned} \frac{dN_{CR}}{dx} &= 2\pi\alpha \left(\frac{1}{\lambda_2} - \frac{1}{\lambda_1} \right) \left[1 - \frac{1}{\beta^2 n^2} \right] \\ &= N_o \left[1 - \frac{1}{\beta^2 n^2} \right] = 0.531 N_o, \end{aligned} \quad (3)$$

where the high-energy limit is used. Over the aforementioned wavelength range, $N_o = 2352 \text{ cm}^{-1}$. Assuming a

constant flux of electrons over the radiator volume V_{rad} , the total path length for all electrons becomes $dx \approx \Gamma_e V_{rad}$. The number of Cherenkov photons produced in the radiator reaching the photocathode is expressed as

$$N_{CRpc} = 0.531 \eta_c K_{sh} N_o \Gamma_e V_{rad}, \quad (4)$$

where η_c is the optical coupling between the radiator and the PMT, and K_{sh} represents flux enhancement from showering that occurs in the material around the radiator. Because the PMT is only a few mm from the open surface of the CD radiator (top surface of Figure 2), η_c is relatively high. The number of photoelectrons generated by the photocathode is $N_{pe} = \eta_Q N_{CRpc}$, where η_Q represents the average quantum efficiency for electron emission from the photocathode over its operating wavelength range. The output charge from the PMT is then

$$Q_{out} = e N_{pe} G(V), \quad (5)$$

where $G(V)$ is the PMT current gain as function of the HV bias V .

OTR

OTR intensity from a single electron per unit frequency and solid angle is given as

$$\frac{d^2 W_O}{d\omega d\Omega} = \frac{e^2}{4\pi^3 \epsilon_o c} \frac{\beta^2 \sin^2 \theta}{(1 - \beta^2 \cos^2 \theta)^2}. \quad (6)$$

Recognizing that $(1 - \zeta^2)^2 = [(1 - \zeta)(1 + \zeta)]^2 \approx 4(1 - \zeta)^2$, where $\zeta = \beta \cos \theta$, Eq. 2 can be written as

$$\frac{d^2 W_O}{d\omega d\Omega} = \frac{e^2}{16\pi^3 \epsilon_o c} \frac{\beta^2 \sin^2 \theta}{(1 - \beta \cos \theta)^2}. \quad (7)$$

Substituting for the solid angle $d\Omega = \sin \theta d\theta d\phi$ and integrating,

$$\begin{aligned} \frac{dW_O}{d\omega} &= \frac{e^2}{16\pi^3 \epsilon_o c} \int_0^{2\pi} d\phi \int_0^{\pi/2} d\theta \frac{\sin^3 \theta}{(1 - \beta \cos \theta)^2} \\ &\approx \frac{e^2}{8\pi^2 \epsilon_o c} [\ln(4\gamma^4) - 3]. \end{aligned} \quad (8)$$

The number of OTR photons generated in the fiber bundle is determined by again integrating over frequency, this time normalizing by the average frequency:

$$N_O = \frac{W_O}{\hbar\omega_{av}} = \frac{e^2}{8\pi^2 \epsilon_o c} [\ln(4\gamma^4) - 3] \frac{2}{\hbar} \frac{\omega_2 - \omega_1}{\omega_2 + \omega_1}. \quad (9)$$

Once again, expressing the number of photons in terms of wavelength and the fine structure constant,

$$N_O = \frac{\alpha}{\pi} [\ln(4\gamma^4) - 3] \frac{\lambda_2 - \lambda_1}{\lambda_2 + \lambda_1}. \quad (10)$$

The wavelength range of the FO PMT in terms of quantum efficiency FWHM is $\lambda_2 = 520 \text{ nm}$ and $\lambda_1 = 320 \text{ nm}$. Assuming full-energy electrons $\gamma = 13,700$, $N_O = 0.0202$.

In the case of OTR, the number of photons will be proportional to the product of the electron flux and the surface area of the fibers; as indicated in Figure 3, this includes the cylindrical area of fibers as well as the ends. The cross-sectional area of the fiber presented to the flux of electrons leaving the beam pipe is the diameter times the length $A_f = d_f l_f$. We assume that the electron fluence is not attenuated appreciably as it travels through the bundle; therefore, each electron that enters a fiber will also exit through the same area. The effective fiber area is then multiplied by 2. The total fiber area then is $2N_f A_f$. The number of OTR photons generated can be expressed as

$$N_{OTR} = 2N_f N_f A_f \Gamma_e. \quad (11)$$

EXPERIMENTAL ARRANGEMENT

The initial installation of an FO beam loss monitor (BLM) prototype started with one fiber bundle in SR Sector 11, placed on the upper side of the downstream straight section vacuum chamber. An FO cable bundle is composed of 61 200- μm , fused-silica fibers in a close-pack arrangement. The effective diameter of the bundle is 2 mm and length is 3 m. The first 30 cm of FO cable was placed directly above the beam centerline. A modified APS SR CD (no lead) was positioned near the bundle as shown in Figure 4.

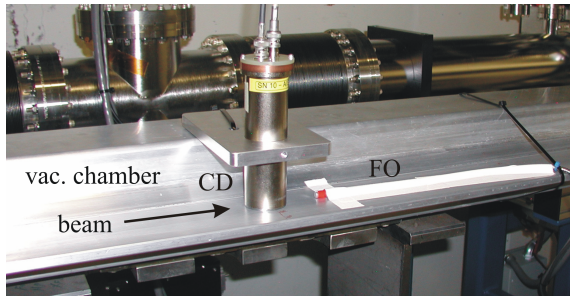


Figure 4: FO and CD loss monitors in Sector 11 IDSS.

Beam loss was recorded with both diagnostics during injection of approximately 2 nC (0.5 mA) into an empty SR. FO and CD BLM traces are shown in Figure 5. The injected beam was stored with the some loss, followed by a total beam dump at 1.4 ms after injection. In this first implementation of the FO BLM, a Burle S83054F PMT was used. R7400U-06 or R5600U PMTs are employed in the APS SR CDs. The gain of the S83054F (3.8×10^5) is about half that of the R7400-06 (7×10^5). In addition, the Burle tube FWHM output is 20 ns for a 1-ns input pulse; whereas the measured width of the R7400-06 is approximately 3 ns.

Signal intensity estimates from the CD and the FO cable detectors are presented in Table 1 for Cherenkov and OTR generation, respectively. Typically, SR injection losses range from 10-20 percent. It is assumed here that 20 percent of the 2 nC of 7-GeV electrons injected into the SR are lost. Approximately half of the injection losses occur in the narrow gap beam pipe in Sector 4; for the purpose of this estimate, it is further assumed that the rest of the lost

Table 1: Comparison of Estimated Cherenkov and OTR Signal Strengths for the CD and FO Detectors

	η_Q	η_c	N_{pe}	Q_{out} (nC)	V_{out} (V)
Cherenkov	0.136	0.5	303	0.034	0.567
OTR	0.32	1.0	10	6.0×10^{-4}	1.5×10^{-3}

charge is distributed uniformly around the ring. Finally, we assume that the loss occurs in 100 equal amplitude pulses.

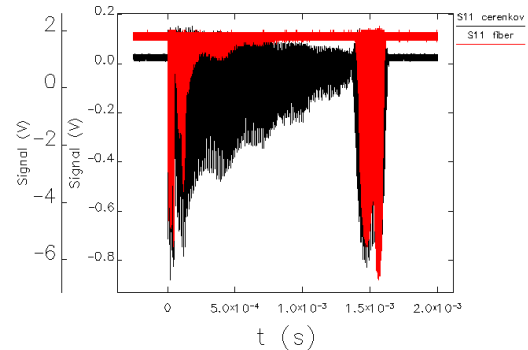


Figure 5: FO and CD BLM signals in Sector 11 IDSS; 2 nC injected followed by a beam dump.

Table 1 shows that OTR in the fibers is still weak relative to Cherenkov light in the CD. However, relative to the data in Figure 5, the CD signals are also low by roughly a factor of 7 ($4\text{V}/0.567\text{V}$). It might be that the electron fluence is actually 7 times larger with 7 times less energy. This factor would be true for the OTR calculation as well; still, this would only bring the OTR signal up to 10 mV, which is low by a factor of roughly 50. Additional enhancement in the OTR signal may be possible due to roughness on the surface of the fibers; given the alignment of the FO cable, this effect could be significant. The lost electron angle after a single scattering event is $1/\gamma = 73 \mu\text{rad}$. Assuming an average angle of 1 mrad, the electron will travel 1 μm in y for each mm in z. If surface roughness on the fiber is 1 μm in height over a length of 2 μm , the electron will cross through this fluctuating index region 500 times.

REFERENCES

- [1] H. Henschel, et al., "Fiber Optic Radiation Sensing Systems for TELSAs," TESLA Report No. 2000-26, Sept. 2000.
- [2] A. Pietryla et al., Proc. of PAC2001, Chicago, June 2001, TPAH304, p. 1622 (2001); <http://www.JACoW.org>.
- [3] E. Janata, Nuc. Instrum. Methods A 493 (2002) 1.
- [4] T. Kawakubo et al., Proc. of EPAC 2004, Lucerne, July 2004, THPLT069, p. 2652 (2004); <http://www.JACoW.org>.
- [5] A. Lumpkin, et al., Nuc. Instrum. Methods A 296 (1990) 150.
- [6] J.D. Jackson, *Classical Electrodynamics*, 2nd ed., Wiley, New York, 1975, p. 639.
- [7] B.X. Yang, private communication.